Published in "Physical Review A 75: 040501(R), 2007"
which should be cited to refer to this work.

Muonic hydrogen cascade time and lifetime of the short-lived 2S state

L. Ludhova,[1,2,*] F. D. Amaro,[3] A. Antognini,[4] F. Biraben,[5] J. M. R. Cardoso,[3] C. A. N. Conde,[3] A. Dax,[2,6,†] S. Dhawan,[6] L. M. P. Fernandes,[3] T. W. Hänsch,[4] V. W. Hughes,[6,‡] P. Indelicato,[5] L. Julien,[5] P. E. Knowles,[1] F. Kottmann,[7] Y.-W. Liu,[8] J. A. M. Lopes,[3] C. M. B. Monteiro,[3] F. Mulhauser,[1,§] F. Nez,[5] R. Pohl,[2,4] P. Rabinowitz,[9] J. M. F. dos Santos,[3] L. A. Schaller,[1] C. Schwob,[5] D. Taqqu,[2] and J. F. C. A. Veloso[3,‖]

[1]*Département de Physique, Université de Fribourg, 1700 Fribourg, Switzerland*
[2]*Paul Scherrer Institut, 5232 Villigen-PSI, Switzerland*
[3]*Departamento de Física, Universidade de Coimbra, 3000 Coimbra, Portugal*
[4]*Max-Planck-Institut für Quantenoptik, 85748 Garching, Germany*
[5]*Laboratoire Kastler Brossel, ENS, UPMC and CNRS, 4 place Jussieu, 75252 Paris Cedex 05, France*
[6]*Physics Department, Yale University, New Haven, Connecticut 06520-8121, USA*
[7]*Institut für Teilchenphysik, ETH Zürich, 8093 Zürich, Switzerland*
[8]*Physics Department, National Tsing Hua University, Hsinchu 300, Taiwan*
[9]*Department of Chemistry, Princeton University, Princeton, New Jersey 08544-1009, USA*

(Received 21 November 2006; published 4 April 2007)

Metastable 2S muonic-hydrogen atoms undergo collisional 2S quenching, with rates which depend strongly on whether the μp kinetic energy is above or below the $2S\rightarrow 2P$ energy threshold. Above threshold, collisional $2S\rightarrow 2P$ excitation followed by fast radiative $2P\rightarrow 1S$ deexcitation is allowed. The corresponding short-lived $\mu p(2S)$ component was measured at 0.6 hPa H_2 room-temperature gas pressure, with lifetime $\tau_{2S}^{\rm short}=165^{+38}_{-29}$ ns (i.e., $\lambda_{2S}^{\rm quench}=7.9^{+1.8}_{-1.6}\times 10^{12}$ s^{-1} at liquid-hydrogen density) and population $\epsilon_{2S}^{\rm short}=1.70^{+0.80}_{-0.56}\%$ (per μp atom). In addition, a value of the μp cascade time, $T_{\rm cas}^{\mu p}=(37\pm 5)$ ns, was found.

Muonic hydrogen ($\mu^- p$) is a simple atomic system, sensitive to basic features of the electromagnetic and weak interactions. Of particular interest is its metastable 2S state, long sought after for measuring the $\mu p(2S)$-Lamb shift $\mathcal{L}_\mu$. Vacuum polarization dominates $\mathcal{L}_\mu$. It shifts the 2S level by 0.2 eV below the 2P level [1,2]. A measurement of $\mathcal{L}_\mu$ is in progress at the Paul Scherrer Institute (PSI), Switzerland [3]. We report here the data analysis of a preliminary stage of this experiment made at low H_2 gas pressure $p_{H_2}=0.6$ hPa [4].

Muons stopped in H_2 gas form highly excited μp atoms [5]. A cascade of both collisionally induced and radiative deexcitations leads to the 1S ground state or, with a probability ϵ_{2S} (few %), to the 2S state. The $\mu p(1S)$ kinetic energy distribution $E_{\rm kin}^{1S}$ has been measured at $p_{H_2}=0.06-16$ hPa [6], and cascade simulations show that $E_{\rm kin}^{1S}$ and $E_{\rm kin}^{2S}$ do not differ significantly under our conditions [5].

The 2S state lifetime is, in the absence of collisions, essentially equal to the muon lifetime $\tau_\mu=2.2$ μs. In H_2 gas, collisional 2S quenching occurs, with different processes for kinetic energies $E_{\rm kin}^{2S}$ above or below the $2S\rightarrow 2P$ transition threshold which is $(1+m_{\mu p}/m_{H_2})|\mathcal{L}_\mu|\approx 0.3$ eV in the laboratory frame.

(i) Most $\mu p(2S)$ atoms are formed at energies above this threshold [6] where a collisional $2S\rightarrow 2P$ Stark transition, followed by $2P\rightarrow 1S$ deexcitation with 1.9 keV $K\alpha$ x ray emission (the 2P lifetime is 8.5 ps),

$$\mu p(2S)+H_2\rightarrow \mu p(2P)+H_2\rightarrow \mu p(1S)+H_2+K\alpha, \quad (1)$$

leads to fast 2S depletion (collisional quenching). A lifetime $\tau_{2S}^{\rm short}\sim 100$ ns$/p_{H_2}$[hPa] was predicted for this *short-lived* 2S component [7–9]. This is too short to have been seen in previous searches for $K\alpha$ x rays delayed with respect to the $\mu p(2S)$ formation time [10–12]. In this Rapid Communication we report on the first measurement of $\tau_{2S}^{\rm short}$ and the corresponding population $\epsilon_{2S}^{\rm short}$.

(ii) Due to elastic collisions, a fraction of the $\mu p(2S)$ atoms decelerates to energies below 0.3 eV where process (1) is energetically forbidden. This fraction is the *long-lived* 2S component. A recent experiment [13] showed that its dominant quenching process is nonradiative deexcitation to the ground state, with lifetime $\tau_{2S}^{\rm long}\approx 1.3$ μs at 0.6 hPa and population $\epsilon_{2S}^{\rm long}\approx 1\%$.

The cascade time $T_{\rm cas}^{\mu p}$ is the mean delay between μp-atom formation and final deexcitation to the ground state [when a μp K-line x ray, other than from $\mu p(2S)$ decay, is emitted]. The $T_{\rm cas}^{\mu p}$ value results from the average of the various cascade deexcitation processes and depends on p_{H_2}. It was calculated [5] but never measured for μp.

In our experiment, muons stop in H_2 gas containing a small admixture of N_2 (air), and we measure simultaneously the three time distributions

---

*Present address: Dipartimento di Fisica, Università degli Studi, via Celoria 16, 20133 Milano, Italy. Electronic address: Livia.Ludhova@mi.infn.it

†Present address: Department of Physics, University of Tokyo, 7-3-1 Hongo, Bunkyo-ku, Tokyo 113-0033, Japan.

‡Deceased.

§Present address: University of Illinois at Urbana-Champaign, Urbana, IL 61801, USA.

‖Present address: Departamento de Física, Universidade de Aveiro, 3819-193 Aveiro, Portugal.

$$K\alpha\text{, i.e., } \mu p(n = 2 \rightarrow 1) \text{ x rays (1.898 keV)},$$

$$K(>\beta)\text{, i.e., } \mu p(n > 3 \rightarrow 1) \text{ x rays [2.45(2) keV[14]]},$$

$$\mu\text{N, i.e., } \mu\text{N}(n = 5 \rightarrow 4) \text{ x rays (3.08 keV[15])}.$$

The $\mu p(n{=}3\rightarrow 1)$ $K\beta$ line (2.249 keV) is not well separated from $K\alpha$ and $K(>\beta)$. The 0.4(1)% air admixture in the H_2 was useful for calibrating x-ray energies and times. The μN time distribution is similar to that of μp formation because the μN cascade time is negligibly short ($\sim 10^{-10}$ s) [16]. The μp cascade time will therefore show up as a time delay in the $K\alpha$ and $K(>\beta)$ distributions compared to μN. The signature for $2S$ radiative decay will be a tail in $K\alpha$ not present in $K(>\beta)$. The muon transfer rates $\mu p + \text{N} \rightarrow \mu\text{N} + p$ are $\sim 10^3$ s^{-1} for $\mu p(1S)$ and $\sim 10^4$ s^{-1} for $\mu p(2S)$ [17], too small to affect our results.

The experiment was performed at the recently developed low-energy μ^- source attached to the πE5 beamline at PSI [18]. It provides $\sim 10^3$ s^{-1} μ^- with energies of a few keV. The muons were axially injected into a 1-m-long, 20-cm-bore solenoid operated at 5 T, containing the muon entrance detectors and the gas target (see [3]). Two detectors, based on nanometer-thick carbon foils, signaled the arrival of slow muons [19]. Muons were stopped in a 20-cm-long target vessel filled with 0.6 hPa H_2 gas (temperature 290 K), and μp atoms were formed in a volume of $0.5 \times 1.5 \times 20$ cm^3. Twenty large-area avalanche photodiodes (LAAPD), each with sensitive area 13.5×13.5 mm^2, were used as x-ray detectors [20]. Muon-decay electrons were detected by a set of plastic scintillators and also by the LAAPDs. More than 5×10^5 events, each where an x ray was followed by an electron, were analyzed.

Calibration data were used for each LAAPD to deduce the energy E_x and time t_x (relative to muon entrance) of a measured x ray. Typical resolutions (full width at half maximum) were $\Delta E_x / E_x \approx 25\%$ and $\Delta t_x \approx 35$ ns for 2-keV x rays. Most μp x rays were found in the time interval $300 \leqslant t_x \leqslant 600$ ns, corresponding to the widely distributed muon slowing-down times.

The $K\alpha$, $K(>\beta)$, and μN time distributions were determined from a fit of the E_x spectra for different t_x intervals. The useful t_x range (0.2–6.5 μs) was divided into 28 intervals (50, 100, and 500 ns wide). For each interval an E_x spectrum was produced. Three typical spectra are shown in Fig. 1, one at times of μp formation and deexcitation (top) and two at later times. The function fit to each spectrum is composed of several x-ray lines and a continuous background. Each line is the sum of a Gaussian peak and a tail toward lower energies (an LAAPD characteristic), with energy-dependent weights [4].

The lines fitted in Fig. 1 correspond to x rays from μp [$K\alpha$, $K\beta$, and $K(>\beta)$], μN (main transitions at 1.67, 3.08, and 6.65 keV [15]), μO (2.19, 4.02, and 8.69 keV), and μC (4.89 keV). The intensities for the $K\alpha$ and $K(>\beta)$ and 3.08-, 4.02-, 4.89-, and 6.65-keV lines were free parameters, whereas the relative intensities of the other lines as well as the positions and widths of all lines were fixed by requiring global consistency for all data [4] and considering known

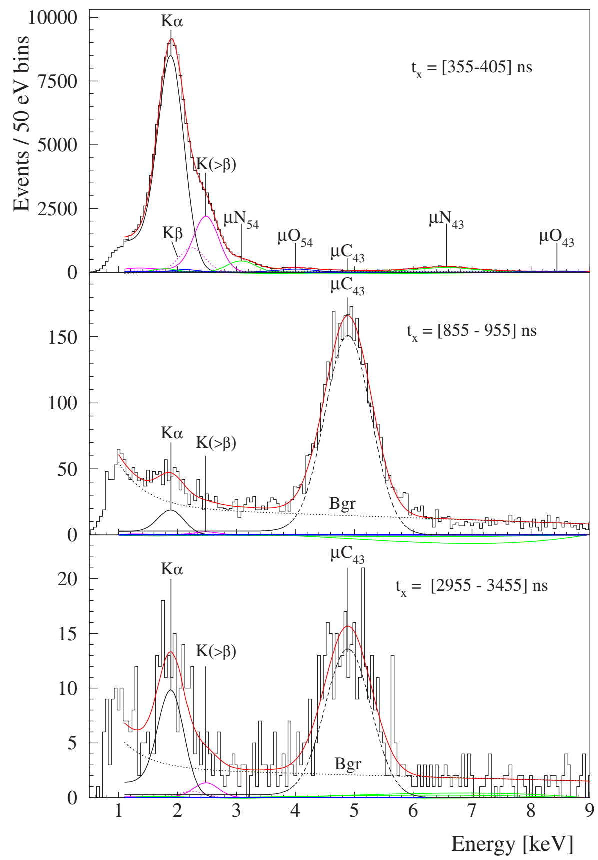

FIG. 1. (Color online) X-ray energy spectra (3 of 28) for different t_x intervals. The fit function is composed of the peaks for μp $K\alpha$, $K\beta$, $K(>\beta)$, μN, μO, and μC (4.89 keV), and a continuous background (Bgr).

yields [21]. The late-time 2-keV peak (see Fig. 1, bottom) is due to μp x rays from *second-muon* stops—i.e., muons entering the target at random times shortly after a *first muon* which defined $t_x{=}0$. The $\mu C_{4\rightarrow 3}$ (4.89 keV) line at late times arises from μp atoms drifting to the polypropylene foils in front of the LAAPDs where muon transfer to C atoms occurred. The continuous background is due to x rays with energy >10 keV, e.g., μC K- and L-line transitions, whose deposited charge was not fully amplified by the LAAPDs. It was well modeled by a sum of an exponential and a linear function, with two amplitudes as free parameters. The full details of the extensive background studies are found in [4].

The fitted intensities (with statistical errors) of the 28 energy spectra are shown in Fig. 2 as a function of t_x, for the three lines μN (3.08 keV), μp $K(>\beta)$, and $K\alpha$. The late-time events are caused by *second-muon* stops. The t_x spectra from different LAAPD positions show [4] that for muons not stopped during their first pass through the gas target, a considerable fraction was reflected at the gold-plated back side of the vessel and stopped during the return pass. Consequently, the μN spectrum (showing the muon stop-time distribution) was represented by a sum of two functions, each one the convolution of a Gaussian with an exponential (Fig. 2, top). The simultaneous fit of the three time spectra, using the common muon stop-time distribution, gives values for the intensities $A_{(\mu\text{N})}$, $A_{(>\beta)}$, and A_{α}.

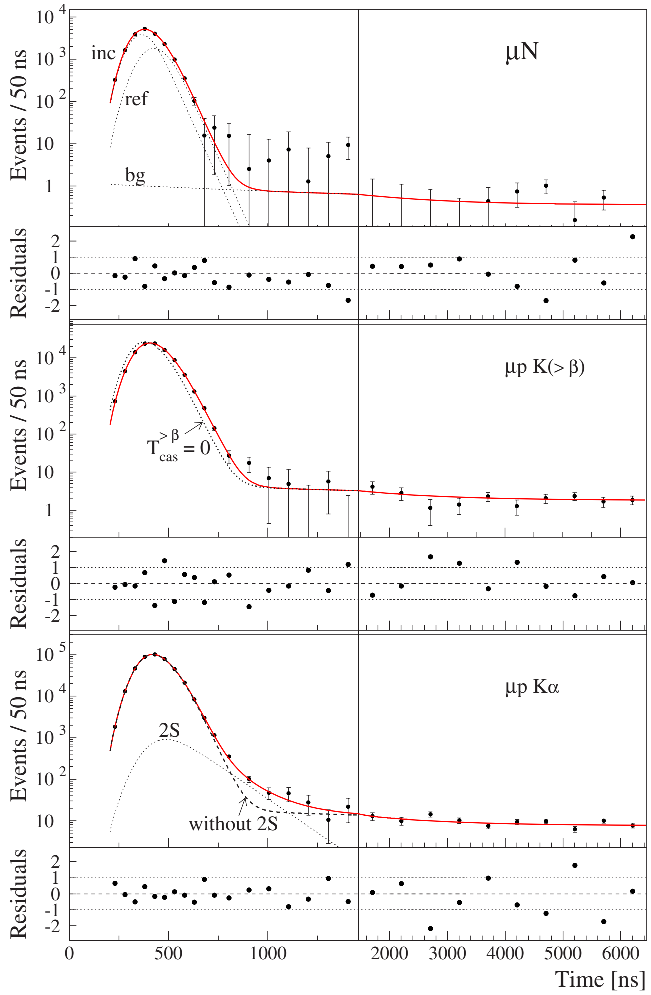

FIG. 2. (Color online) Fit functions (solid line) and residuals (normalized by the errors) for fits to the x-ray time spectra for the lines μN (3.08 keV) (top), $\mu p - K(>\beta)$ (middle), and $K\alpha$ (bottom). Each point results from a fit of the x-ray energy spectrum for the corresponding t_x interval (50, 100, and 500 ns wide). The dotted lines in the μN spectrum are the functions for incoming (inc), reflected (ref), and *second* (bg) muons. In the $K(>\beta)$ spectrum the dotted line is the fit function without cascade time. In the $K\alpha$ spectrum the $2S$ tail—i.e., the contribution of the short-lived $\mu p(2S)$ state—is shown as the dotted line. The dashed line is the fit function minus the $2S$ tail.

The $K(>\beta)$ and $K\alpha$ spectra are delayed and slightly broadened with respect to μN due to the μp cascade time. It is not possible to extract the precise shape of the cascade time distribution from the data, but calculations [5] indicate that the $K(>\beta)$ cascade has an approximately exponential time distribution, whereas the $K\alpha$ cascade has the same asymptotic form, but includes growth behavior at earlier times. The μN fit function was therefore convoluted with an exponential (parameter $\tau_{\rm cas}$) to obtain the $K(>\beta)$ function and further convoluted with a Gaussian (parameter $\sigma^{\alpha}_{\rm cas}$) for the $K\alpha$ function. In addition, free time offsets $\Delta T_{(>\beta)}$ and ΔT_{α} [for $K(>\beta)$ and $K\alpha$, with respect to μN] were introduced. The contribution of the short-lived $\mu p(2S)$ state was considered by adding to the $K\alpha$ function a convolution of the $K(>\beta)$ distribution with an exponential (parameter $\tilde{\tau}^{\rm short}_{2S}$) and a relative population $\tilde{\varepsilon}^{\rm short}_{2S}$ (normalized for the fit to A_{α}).

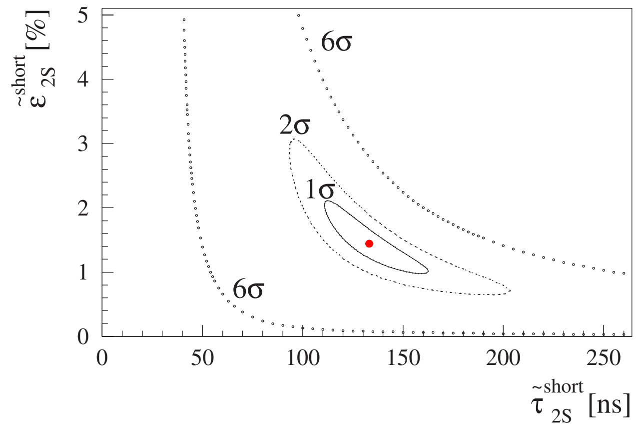

FIG. 3. (Color online) Relative population $\tilde{\varepsilon}^{\rm short}_{2S}$ (normalized to A_{α}) of the short-lived $\mu p(2S)$ component versus its lifetime $\tilde{\tau}^{\rm short}_{2S}$ (without systematic corrections). The dot represents the best fit.

A simultaneous fit of the three time spectra was performed, resulting in $\chi^2 = 57.5$ for 67 degrees of freedom. The fit functions and residuals are shown in Fig. 2. The scatter of the residuals confirms that no relevant systematic deviations exist between the data and the model. The resulting cascade time slope is $\tau_{\rm cas} = (26 \pm 2)$ ns. The time shift $\Delta T_{(>\beta)} = (0 \pm 5)$ ns is consistent with zero, as expected for the $K(>\beta)$ cascade, whereas $\Delta T_{\alpha} = (13 \pm 5)$ ns and $\sigma^{\alpha}_{\rm cas} = (15 \pm 2)$ ns approximate a $K\alpha$ cascade time distribution which deviates from an exponential in the first ~ 20 ns. The deduced mean cascade times $T^{(>\beta)}_{\rm cas} = \tau_{\rm cas} + \Delta T_{(>\beta)} = (26 \pm 5)$ ns and $T^{\alpha}_{\rm cas} = \tau_{\rm cas} + \Delta T_{\alpha} = (39 \pm 5)$ ns, weighted by the corresponding K-line yields, result in a mean μp cascade time $T^{\mu p}_{\rm cas} = (37 \pm 5)$ ns. [The relative K yields at $p_{H_2} = 0.6$ hPa were deduced from [14] as $Y_{\alpha} = 0.821(12)$, $Y_{\beta} = 0.061(9)$, and $Y_{(>\beta)} = 0.118(11)$, and the $K\beta$ cascade time was assumed to be equal to $T^{(>\beta)}_{\rm cas}$.] $T^{\mu p}_{\rm cas}$ depends only weakly on the fit function details because it essentially reproduces the center-of-gravity shifts of the $K\alpha$ and $K(>\beta)$ distributions relative to μN.

The fit results for the $2S$ tail are $\tilde{\tau}^{\rm short}_{2S} = 133^{+29}_{-22}$ ns and $\tilde{\varepsilon}^{\rm short}_{2S} = 1.44^{+0.67}_{-0.46}\%$. As shown in Fig. 3, the absence of the $2S$ tail, corresponding to $\tilde{\varepsilon}^{\rm short}_{2S} = 0$, is excluded by 6σ. As a test, the $K(>\beta)$ spectrum was also fit with a "$2S$" tail. Its amplitude $\varepsilon_{(>\beta)}$ [normalized to $A_{(>\beta)}$] is compatible with zero (within 0.7σ) for any $\tilde{\tau}^{\rm short}_{2S}$, as expected. We conclude that our fit function correctly reproduces the muon stop, cascade, and *second-muon* time distributions. The difference between $\tilde{\varepsilon}^{\rm short}_{2S}$ and $\varepsilon_{(>\beta)}$ is $\tilde{\varepsilon}^{\rm short}_{2S} - \varepsilon_{(>\beta)} = (1.36 \pm 0.28)\%$ at $\tilde{\tau}^{\rm short}_{2S} = 133$ ns. A zero value of this difference is excluded by $\geqslant 4.4\sigma$ for any $\tilde{\tau}^{\rm short}_{2S}$, confirming that the tail in the $K\alpha$ spectrum can only come from $2S$ quenching.

The measured $\tilde{\tau}^{\rm short}_{2S}$ and $\tilde{\varepsilon}^{\rm short}_{2S}$ values have to be corrected for several effects. The necessary corrections were deduced from a Monte Carlo simulation of the experiment, based on the known distribution of $E^{2S}_{\rm kin}$ [6] and on calculated cross sections [9] for process (1) and elastic collisions. It was found that (i) some $\mu p(2S)$ atoms reach the target walls before being quenched; (ii) the solid angle for $K\alpha$ detection varies with time due to the $\mu p(2S)$ motion; (iii) because of collisions, the $E_{\rm kin}^{2S}$ distribution depends on time and hence so do the mean cross sections and μp velocities. Those effects modify the $2S$ tail shape at the late times where the experiment is most sensitive. The resulting correction factors are 1.24 ± 0.07 for $\tilde{\tau}_{2S}^{\rm short}$ and 1.34 ± 0.09 for $\tilde{\varepsilon}_{2S}^{\rm short}$. In addition, $\tilde{\varepsilon}_{2S}^{\rm short}$ has to be multiplied by $(1-\tau_{2S}^{\rm short}/\tau_{\mu})^{-1}$ to account for muon decay and by $Y_{\alpha}/(1+\varepsilon_{2S}^{\rm long})$ to normalize to all μp atoms. The final result for the radiative lifetime and population of the short-lived $\mu p(2S)$ component at 0.6 hPa (temperature 290 K) is $\tau_{2S}^{\rm short}=165_{-29}^{+38}$ ns and $\varepsilon_{2S}^{\rm short}=1.70_{-0.56}^{+0.80}\%$.

The results of our experiment can be discussed as follows: (i) The μp cascade time and the $2S$ tail have been disentangled from the stop-time distribution for the first time. This has been made possible by the high statistics, the low gas pressure, and the good stop-time resolution. The measured μp cascade time $T_{\rm cas}^{\mu p}=(37\pm5)$ ns is less than half the ≈ 90 ns value predicted for 0.6 hPa by cascade calculations [5]. The measured value may be slightly affected by a possible difference in the μ^- atomic capture times of N_2 and H_2 predicted by some models [22]: the muon energy from which capture occurs is expected to increase with Z [23], so μN atoms can form earlier than μp atoms during the muon stopping, an effect which would result in an even lower measured $T_{\rm cas}^{\mu p}$ value. A result which does not depend on such effects is the measured difference $T_{\rm cas}^{\alpha}-T_{\rm cas}^{(>\beta)}=(13\pm4)$ ns, also significantly smaller than the calculated value of ≈ 25 ns. The calculated cascade times may be too long since Coulomb deexcitations, which dominate the cascade at high n levels even at low p_{H_2} [5], may be accompanied by *simultaneous* Auger transitions, an effect not yet considered. (ii) We have compared the measured radiative $2S$ lifetime with the results of calculations. Since the existing calculated cross sections neglect molecular effects, we allowed for the extreme cases where the H_2 molecule is taken as two separate H atoms or as a single atom. Analyzing the simulated data in the time region where the experiment is sensitive, we obtained a value of (178 ± 30) ns which agrees well with the experimental result $\tau_{2S}^{\rm short}=165_{-29}^{+38}$ ns. This confirms the validity of the cross sections calculated for $\mu p(2S)+{\rm H}\rightarrow\mu p(2P)+{\rm H}$ Stark transitions [8,9]. The quenching rate for the short-lived $2S$ component, when normalized to liquid-hydrogen atom density (LHD, 4.25×10^{22} atoms/cm^3), is $\lambda_{2S}^{\rm quench}({\rm LHD})=7.9_{-1.6}^{+1.8}\times10^{12}\ {\rm s}^{-1}$, $\sim$20 times faster than for the long-lived one [13]. (iii) The sum of the measured relative populations $\varepsilon_{2S}^{\rm short}=1.70_{-0.56}^{+0.80}\%$ and $\varepsilon_{2S}^{\rm long}\approx1\%$ (extrapolated to 0.6 hPa, from [13]) is $(2.7\pm0.8)\%$, in agreement with the total $2S$ population $\varepsilon_{2S}=(2.49\pm0.17)\%$ at 0.6 hPa deduced directly from the measured μp K-line yields [14]. We conclude that there is now good understanding of both the short- and long-lived $\mu p(2S)$ dynamics.

We thank L.M. Simons and B. Leoni for setting up the cyclotron trap, O. Huot and Z. Hochman for technical support, and T.S. Jensen for fruitful discussions. We also thank the PSI accelerator division, the Hallendienst, and the workshops at PSI, MPQ, and Fribourg for their valuable help. This work was supported by the Swiss National Science Foundation, the French-Swiss program "Germaine de Staël" (PAI No. 07819NH), the BQR de l'UFR de physique fondamentale et appliquée de l'Université Paris 6, the Portuguese FCT and FEDER under Project No. POCTI/FNU/41720/2001, and the U.S. Department of Energy.

[1] K. Pachucki, Phys. Rev. A **53**, 2092 (1996).
[2] M. I. Eides, H. Grotch, and V. A. Shelyuto, Phys. Rep. **342**, 63 (2001).
[3] R. Pohl *et al.*, Can. J. Phys. **83**, 339 (2005).
[4] L. Ludhova, Ph.D. thesis, Université de Fribourg, Switzerland, 2005, available at http://ethesis.unifr.ch/theses/.
[5] T. S. Jensen and V. E. Markushin, Eur. Phys. J. D **21**, 271 (2002); T. S. Jensen (private communication).
[6] R. Pohl, Ph.D. thesis 14096, ETH Zurich, 2001.
[7] G. Kodosky and M. Leon, Nuovo Cimento Soc. Ital. Fis., B **1B**, 41 (1971).
[8] G. Carboni and G. Fiorentini, Nuovo Cimento Soc. Ital. Fis., B **9B**, 281 (1977).
[9] T. S. Jensen and V. E. Markushin, e-print nucl-th/0001009.
[10] H. Anderhub *et al.*, Phys. Lett. **71**B, 443 (1977).
[11] P. O. Egan *et al.*, Phys. Rev. A **23**, 1152 (1981).
[12] J. A. Böcklin, Ph.D. thesis 7161, ETH Zurich, 1982.
[13] R. Pohl *et al.*, Phys. Rev. Lett. **97**, 193402 (2006).
[14] H. Anderhub *et al.*, Phys. Lett. **143B**, 65 (1984).
[15] P. Hauser, K. Kirch, F. Kottmann, and L. M. Simons, Nucl. Instrum. Methods Phys. Res. A **411**, 389 (1998).
[16] L. Bracci and G. Fiorentini, Nuovo Cimento Soc. Ital. Fis., A **43A**, 9 (1978).
[17] L. Bracci and G. Fiorentini, Nuovo Cimento Soc. Ital. Fis., A **50A**, 373 (1979).
[18] A. Antognini *et al.*, in *Low Energy Antiproton Physics*, edited by D. Grzonka *et al.*, AIP Conf. Proc. No. 796 (AIP, Melville, NY, 2005), p. 253.
[19] M. Mühlbauer *et al.*, Hyperfine Interact. **119**, 305 (1999).
[20] L. Ludhova *et al.*, Nucl. Instrum. Methods Phys. Res. A **540**, 169 (2005).
[21] K. Kirch *et al.*, Phys. Rev. A **59**, 3375 (1999).
[22] J. S. Cohen, Rep. Prog. Phys. **67**, 1769 (2004).
[23] J. S. Cohen, Phys. Rev. A **65**, 052714 (2002).